University of Nebraska - Lincoln

DigitalCommons@University of Nebraska - Lincoln

2015

Chirally-sensitive electron-molecule interactions

J. M. Dreiling

Timothy J. Gay

Chirally-sensitive electron-molecule interactions

JM Dreiling[1] **and TJ Gay**

Jorgensen Hall, University of Nebraska, Lincoln, Nebraska 68588-0299, USA

E-mail: `jmdreiling2@gmail.com`

Abstract.   All molecular forms of life have chemically-specific handedness. However, the origin of these asymmetries is not understood. A possible explanation was suggested by Vester and Ulbricht immediately following the discovery of parity violation in 1957: chiral beta radiation in cosmic rays may have preferentially destroyed one enantiomeric form of various biological precursors. In the experiments reported here, we observed chiral specificity in two electron-molecule interactions: quasi-elastic scattering and dissociative electron attachment. Using low-energy longitudinally spin-polarized (chiral) electrons as substitutes for beta rays, we found that chiral bromocamphor molecules exhibited both a transmission and dissociative electron attachment rate that depended on their handedness for a given direction of incident electron spin. Consequently, these results, especially those with dissociative electron attachment, connect the universal chiral asymmetry of the weak force with a molecular breakup process, thereby demonstrating the viability of the Vester-Ulbricht hypothesis.

1. Introduction

Many biological molecules exist in nature with only one chirality [1]. However, the exact origin of this enantiomeric imbalance is not known. One theory that attempts to explain this ubiquitous biological homochirality is the Vester-Ulbricht hypothesis [2,3], which identifies the left-handed electrons produced in parity-violating beta radiation as the source of the initial imbalance. Vester and Ulbricht suggested that these electrons interacted with precursors of biological molecules and preferentially destroyed one handedness. Specifically, their prediction was that the bremsstrahlung radiation produced by the slowing chiral electrons was responsible for the asymmetry [3]. An extension of this idea is that the chiral electrons themselves are responsible for the enantio-specific destruction.

Experiments searching for such a chirally-sensitive effect due to beta radiation, or the laboratory-equivalent, longitudinally spin-polarized electrons, have been characterized by negative results and/or irreproducibility [4–8]. Some experiments have had more success in demonstrating chiral selectivity [9–12]. However, they do not specify what mechanism is responsible or if the destruction is due to the electrons themselves or subsequent polarized bremsstrahlung. There are several comprehensive, critical reviews of the literature in this area [5,6,13].

Our experiments were performed with longitudinally-spin polarized electrons in place of the beta rays and unoriented gas phase target molecules of 3-bromocamphor ($C_{10}H_{15}BrO$). Such experiments provide several desirable consequences. First, any asymmetries that arise with an

---

unoriented gas-phase target must be due to the chirality of the projectile and the target, whereas in a condensed matter experiment, there is the potential for complications due to, e.g., a residual chiral geometry associated with the target and its mechanical support structure. Additionally, the gas phase permits better identification of the entrance and exit reaction channels. Our experimental setup also allows for varying the incident electron energy, including keeping the electron energy very low so that photolysis due to bremsstrahlung is negligible.

We considered two different chiral electron/chiral molecule interactions. The first is associated with transmission of spin-polarized electrons through chiral molecules. In this experiment, the current transmitted through the gas of molecules is monitored, and an asymmetry is detected by measuring an electron helicity-dependence of this current. The current is, in turn, dependent on the quasi-elastic total cross section for e^--bromocamphor scattering. This experiment has already been performed by the Münster group [14, 15]. Given the significance of their result, which gave the first indication of chiral sensitivity in electron-molecule scattering, it was important that it be reproduced. The second type of experiment considers the rate of dissociative electron attachment (DEA) [16] in bromocamphor. This reaction can be represented by

$$\mathrm{e}^- + \mathrm{C_{10}H_{15}BrO} \longrightarrow \mathrm{C_{10}H_{15}O}^\bullet + \mathrm{Br}^-.$$

In DEA, a temporary negative ionic state is formed, causing an increased interaction time between the incident electron and the chiral molecule. This allows the incident helical electron and the chiral molecule to "sample each others chirality" during the anion's lifetime, which might therefore enhance chiral sensitivity in the breakup rates [17]. Bromocamphor is a good candidate for a DEA asymmetry study as it has been measured to have a very large DEA cross section at near-zero incident electron energy [18]; low incident electron velocities should further enhance any "chirality sampling" effects. Important work on DEA [19–22] has illustrated the vital role of achiral electrons in biologically-important bond-breaking interactions. We were able to successfully measure a chiral asymmetry in the DEA process as manifested by an electron-spin-dependent negative ion current [23]. This constitutes an unambiguously identified chirally-sensitive molecular breakup process and, as such, provides circumstantial evidence for the Vester-Ulbricht hypothesis.

2. Methods

Our experimental apparatus, shown in Fig. 1, has four main components: a spin-polarized electron source, a target chamber, an optical electron polarimeter, and an active-feedback optical system. The latter is not included in Fig. 1 but is discussed in detail in [24]. The source of spin-polarized electrons is a negative-electron-affinity (NEA) GaAs photocathode [25], in which the electrons' longitudinal polarization is determined by the helicity of incident laser light. The optical setup used to produce the circularly polarized light for photoemission of spin-polarized electrons also allows for active feedback to reduce instrumental asymmetries [24]. Solenoidal magnets (also shown in Fig. 1) are used to produce a magnetic field of ~ 15 mT which helps to guide the electron beam out of the source and around a bend in the differential pumping chamber before entering the target chamber. The target chamber is arranged to allow electron polarization measurement with an optical polarimeter [26]. We measured our electron polarization to be constant at $\sim 30\%$ throughout the duration of our chiral asymmetry measurements.

The details of the electron optic elements in the target chamber are shown in Fig. 2. The incident electron energy is determined by performing a retarding field analysis (RFA) [27] in which the voltage applied to the inner and outer target cells and elements 4 and 5 are all ramped simultaneously. The transmitted current is monitored on the Faraday cup (FC), and 0 eV electron energy is defined to correspond to the peak in the derivative of the current collected on the FC, as shown in Fig. 3. The energy scale is linear in the retarding voltage placed on the
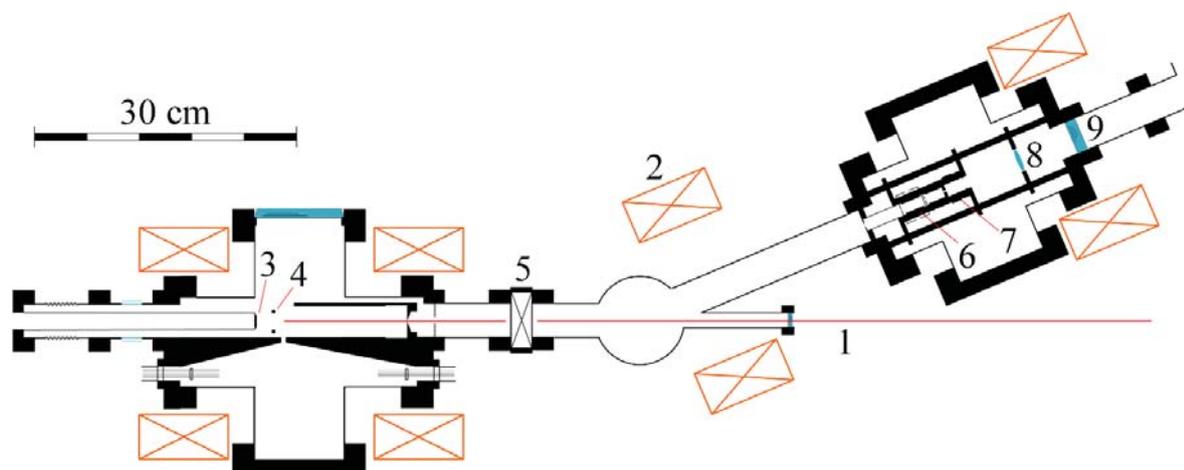
Figure 1. Polarized electron source and target chamber. (1) laser beam from active feedback system to produce GaAs photoemission; (2) solenoidal guiding magnets; (3) GaAs photocathode; (4) NEA activation cesiators; (5) gate valve; (6) chiral target cell (see also Fig. 2); (7) optical polarimeter target cell; (8) fluorescence collection lens; (9) window for the optical polarimeter. The bend in the apparatus eliminates the line-of-sight between the target cell and the GaAs crystal to minimize chemical contamination of the NEA photocathode. Figure from ref. [23].
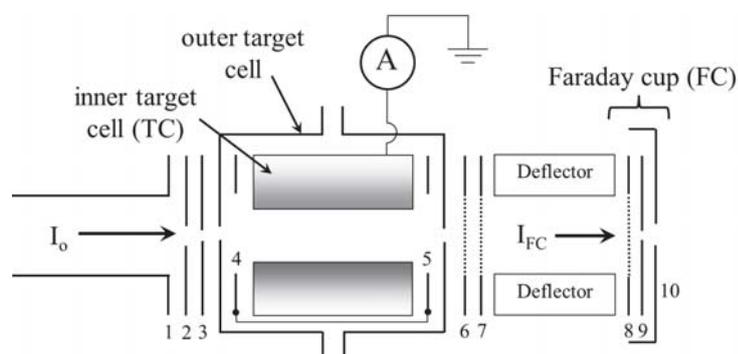

Figure 2. Details of the target vapor cell, showing the incident (I_o) and transmitted (I_{FC}) electron beams, the target cell structure, lens elements 1-10, and the Faraday cup assembly used to measure the transmitted beam. Based on figure from ref. [23].

target cell, and "negative" energies correspond to the high energy tail of the incident electron beam, which had a nominally Gaussian profile and a FWHM energy width of ~ 0.6 eV. In the energy range considered, the average incident electron kinetic energy in the target varies monotonically but non-linearly with the retarding potential. At the most positive energy values, the beam's FWHM is the full 0.6 eV; at potentials less than zero, the energy spread in the target region approaches zero as does the average kinetic energy.

During a chiral asymmetry measurement, molecules of a given handedness are admitted into the target cell (Figs. 1 and 2). The pressures used depend on whether we are measuring DEA or transmission asymmetries. Unscattered electron beam current is detected on the FC following the target cell, and anion current is measured on the electrically-isolated inner target cell wall. As previously mentioned, a magnetic field of ~ 15 mT is directed along the axis of the apparatus. This guides the electrons through the target cell and onto the FC. Thus, scattered electrons are largely prevented from reaching the inner walls of the target cell. Anions, with their larger mass, have larger radii of curvature through the magnetic field and are therefore able to drift to the target cell walls where they are detected as a current. Electron-spin-dependent asymmetries are determined by using a lock-in amplifier to detect the change in currents (collected on the FC
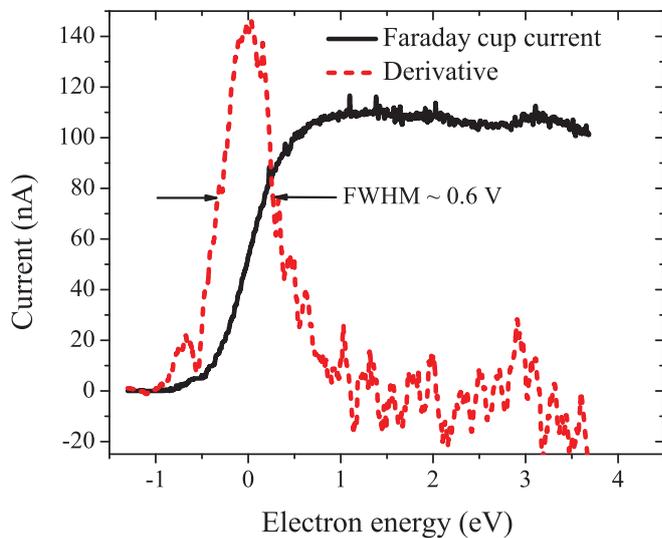
Figure 3. Retarding field analysis (RFA) scan showing the current collected on the Faraday cup. Electron energy is defined such that 0 eV corresponds to the peak in the derivative of the RFA scan (see text).

for transmission and on the inner target cell walls for DEA) at the frequency of the electron helicity reversal.

3. Results
3.1. Transmission asymmetries

To take transmission asymmetry data, chirally-pure bromocamphor was admitted to the target cell until the incident electron beam at the energy of the asymmetry measurement was attenuated by about 70%. This corresponded to a bromocamphor pressure of 2.0–3.0 mTorr, depending on the incident electron energy, as measured by a capacitance manometer. Multiple scattering has a negligible effect on our measured asymmetries because it does not significantly alter the electron beam polarization. The electron helicity was reversed at a frequency of $\sim$210 Hz, and the FC current asymmetry associated with the helicity reversal, $a = (I_\uparrow - I_\downarrow)/(I_\uparrow + I_\downarrow)$, was monitored for ~ 3 minutes using a lock-in amplifier. Here, $I_\uparrow$ ($I_\downarrow$) is the current measured for spin-forward (spin-backward) electrons collected on the FC. Thus, a_L and a_R are the electron-helicity-dependent components of the transmission signal for the L- and R-enantiomers of bromocamphor, respectively. The chirality of the target gas was then switched and data collected again. A final asymmetry value A was calculated using

$$A = a_L - a_R = \left[\frac{I_\uparrow - I_\downarrow}{I_\uparrow + I_\downarrow}\right]_L - \left[\frac{I_\uparrow - I_\downarrow}{I_\uparrow + I_\downarrow}\right]_R. \tag{1}$$

This formulation compensates for persistent instrumental asymmetries that are common between the measurements for both enantiomers. At each energy, A was measured ~ 20 times and an average was found after applying Chauvenet's criterion [28] to the data.

As previously mentioned, asymmetry measurements of the transmission of spin-polarized electrons through chiral bromocamphor have already been performed by the Münster group [14, 15]. However, their data were taken under different experimental conditions, including different electron polarization (40%), electron beam attenuation (90%), and electron energy width (0.3 eV) [14]. We therefore must rescale the data from ref. [15] in order to obtain a comparison with our data. It is straightforward to show [14] that for transmission

$$a \approx P \ln\left(\frac{I(P=0)}{I_o}\right)\left(\frac{\sigma_\uparrow - \sigma_\downarrow}{\sigma_\uparrow + \sigma_\downarrow}\right), \tag{2}$$
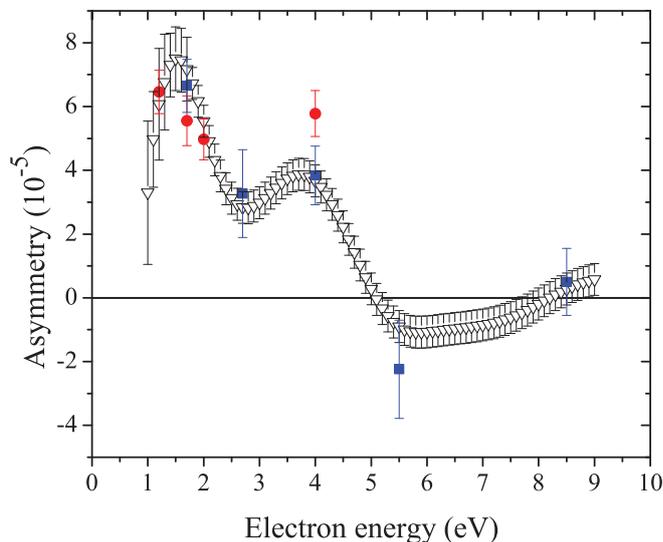
Figure 4. The asymmetry in the transmitted current collected on the FC as a function of electron energy. Squares and circles represent our measurements; the triangles are the measurements of Nolting *et al.* [15] scaled to our experimental parameters and our definition of asymmetry (see text). The difference between the squares and circles corresponds to flipping the setting of the quarter-wave plate that circularly polarizes the laser light [24], which should give measurements of opposite sign. The sign of the data represented by circles has been reversed for easier comparison to the data of Nolting *et al.* [15]. Uncertainties are determined by taking the standard deviation of the mean of the individual asymmetry measurements.

where P is the electron polarization, I_o is the unattenuated incident current, $I(P = 0)$ is the transmitted current with an unpolarized electron beam, and $\sigma_\uparrow$ and $\sigma_\downarrow$ represent the quasi-elastic cross sections for spin-forward and spin-backward electrons, respectively.

First, in order to match our definition of asymmetry, we calculated

$$A_M = (a_M)_L - (a_M)_R, \tag{3}$$

where a_M is the Münster data from Nolting *et al.* [15]. Next, to compensate for the differences of electron beam polarization and attenuation, a scaling of

$$A'_M = A_M \left(\frac{0.3}{0.4}\right) \left(\frac{\ln(0.3)}{\ln(0.1)}\right) \tag{4}$$

was applied. Finally, the data was convoluted to account for the differences in the electron-beam energy widths for the two experiments. The results are presented in Fig. 4 along with our data. Although our measurements are more sparsely distributed in energy, they are in good agreement with the previous measurements.

As a systematic check, the data were taken using two different settings of the quarter-wave plate that polarizes the laser light. This essentially introduces a phase-shift of π in the measurement, as it reverses the sign of the electron polarization for a given optical configuration. Thus, the sign of the asymmetry is reversed. In Fig. 4, we plot these data mulplied by -1 in order to make the comparison to ref. [15] more apparent.

3.2. DEA asymmetries
The DEA asymmetry measurements were taken in essentially the same way as transmission measurements, with a few notable differences. The DEA data were taken with bromocamphor introduced into the target cell such that the incident 0 eV electron beam was attenuated to $\sim 50\%$ of its initial value, which required a pressure of 0.5–1.0 mTorr. Asymmetry measurements of DEA were taken by monitoring the anion current collected on the inner target cell wall (see
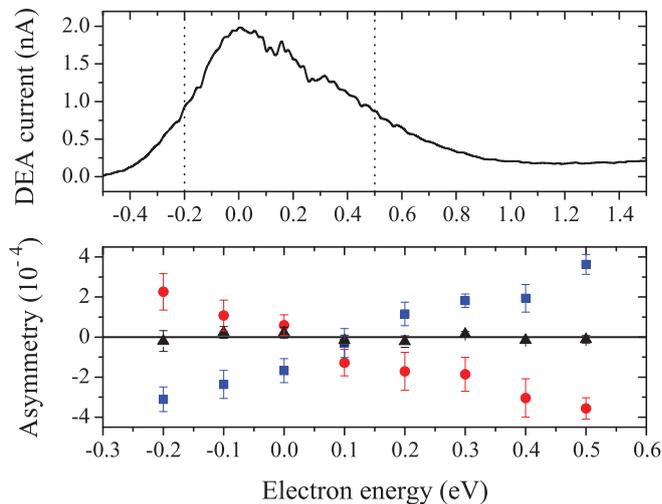
Figure 5. Top: DEA current, with the range of energies where asymmetry data were taken indicated by the dotted vertical lines. Bottom: The asymmetry in DEA current as a function of electron energy. Squares and circles represent opposite settings of the quarter-wave plate that circularly polarizes the laser light, which should give asymmetry measurements of opposite signs. A positive sign for the data represented as squares corresponds to a positive sign for the data of Nolting *et al.* [15] with (−) bromocamphor. The triangles indicate data taken with racemic bromocamphor. Uncertainties are determined by taking the standard deviation of the mean of the individual asymmetry measurements. Figure from ref. [23].

Fig. 2). Thus $I_\uparrow$ ($I_\downarrow$) in Eq. 1 was the current measured on the inner target cell walls when the incident electron helicity was spin-forward (spin-backward).

Figure 5 shows the DEA signal and its asymmetry for a range of electron energies near 0 eV. Our measurements of non-zero asymmetries indicate that we are detecting an electron-helicity-dependent break-up of chiral molecules. *As such, they validate the Vester-Ulbricht hypothesis, which connects the origins of biological homochirality with helical beta radiation.*

Again, a systematic check was done by taking asymmetry measurements with opposite settings of the final quarter-wave plate. An additional check was performed by collecting asymmetry data using two samples of racemic bromocamphor. Because these samples have no net chirality, they should result in zero asymmetry. Data were taken exactly as before, with a recorded for each of the samples and A calculated by finding the difference. (In this situation, the subscripts are arbitrary.) This measurement yielded asymmetries consistent with zero.

3.3. Contribution of scattered electrons to DEA asymmetries

During the DEA measurements, we measured the current detected on the inner target cell walls (Fig. 2). A potential concern here is that, in addition to anions produced in a DEA reaction, scattered electrons might be detected on the inner target cell walls. This problem is exacerbated as the beam energy approaches zero. Although the longitudinal magnetic field should largely eliminate the electron background, it only reduces it to a manageable level. To estimate its contribution to the target cell wall current, we performed a systematic study by comparing the current detected on the inner target cell walls for both bromocamphor and nitrogen over the range of energies of the DEA asymmetry data. While bromocamphor has an appreciable DEA cross-section at near-zero energy, nitrogen does not. Therefore, the current detected on the inner target cell walls when nitrogen is in the target cell serves as a measure of the inner target cell collection efficiency of scattered electrons and therefore the contribution of scattered electrons to the inner target cell wall current.

Our estimation of α, the scattered electron contribution to our inner target cell wall current, is shown in Fig. 6 as a function of C_{DEA}, the assumed collection efficiency of anions produced
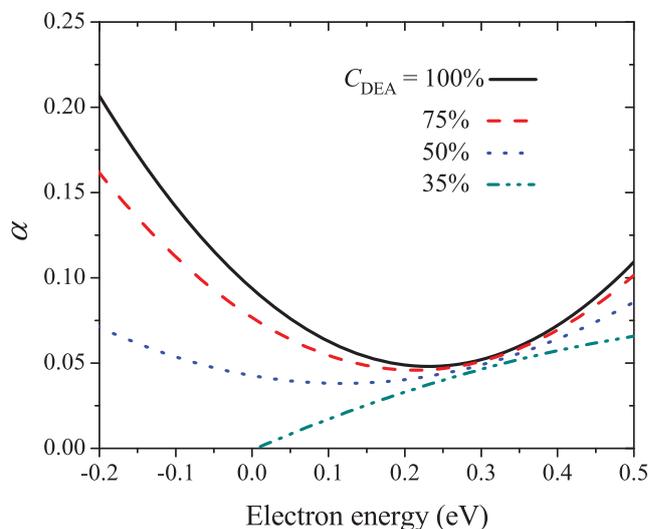
Figure 6. Component of the inner target cell current due to scattered electrons, α, as a function of target retarding voltage for different assumptions about C_{DEA}, the collection efficiency of DEA anions. The curves represent quadratic fits to the data, which are distributed about their respective fits with a standard deviation of ~ 0.03. Figure from ref. [23].

by DEA. Details of the analysis are given in ref. [23]. We determined the scattered electron contribution to be largest at -0.2 eV (assuming $C_{DEA} = 100\%$), where it is at most $\sim 20\%$ of the total current. It drops to an upper limit of 7% as the energy increases to 0.1 eV and rises slowly to at most 10% at 0.5 eV. Thus, the asymmetries measured above 0 eV likely represent our most accurate determination of the true chiral DEA asymmetry.

4. Conclusions

Our experiment has demonstrated chirally-sensitive asymmetric breakup of bromocamphor by near 0 eV incident spin-polarized electrons in a DEA reaction. These measurements thus provide important, although circumstantial, evidence for the Vester-Ulbricht hypothesis [2, 3]. We have also confirmed the asymmetries associated with quasi-elastic scattering measured by the Münster group [14, 15].

We are unaware of any calculations that have predicted the expected size of chiral asymmetries for real molecules (as opposed to simplified models) in either quasi-elastic or DEA channels. Therefore, our interpretation of the energy dependence of the size of the asymmetry is only speculative. In considering the transmission results (Fig. 4), the asymmetry is appreciable only at the lower energies. This suggests that resonances are important in determining the sizes of the asymmetry [29, 30]. For the DEA results shown in Fig. 5, it is reasonable to expect that the scattered electrons, in addition to the anions, detected on the inner target cell walls contribute to the measured asymmetry. This would show up primarily at the lowest energies investigated, as this is where the scattered electron contribution is the largest. In light of this, the asymmetries measured at the highest energies probably provide the most accurate representations of the DEA asymmetry. The fact that the DEA asymmetries are substantially larger than the transmission asymmetries is perhaps not surprising, considering the fact that in DEA a temporary negative ion is produced, thereby increasing the interaction time between the spin-polarized electron and the chiral molecule and allowing the two more opportunity to "sample each others chirality."

References

[1] Evans AC, Meinert C, Giri C, Goesmann G and Meierhenrich UJ 2012 Photochemistry and the detection of amino acids in interstellar ice analogues and comets. *Chem. Soc. Rev.* **41** 5447

[2] Vester F, Ulbricht TLV and Krauch H 1959 Optical activity and parity violation in β-decay. *Naturwissenschaften* **46** 68

[3] Ulbricht TLV and Vester F 1962 Attempts to induce optical activity with polarized β-radiation. *Tetrahedron* **18** 629

[4] Fitz D, Reiner H, Plankensteiner K and Rode BM 2007 Possible origins of biohomochirality. *Current Chemical Biology* **1** 41

[5] Bonner WA 2000 Parity violation and the evolution of biomolecular homochirality. *Chirality* **12** 114-26

[6] Bonner WA 1991 The origin and amplification of biomolecular chirality. *Orig. Life Evol. Biosphere* **21** 59111

[7] See, e.g., Hodge LH, Dunning FB and Walters GK 1979 Degradation of DL-leucine with longitudinally polarized electrons. *Nature* **280** 250-2

[8] See, e.g., Bonner WA, Blair NE and Flores JJ 1979 Attempted asymmetric radiolysis of D,L-tryptophan with ^{32}P β-radiation. *Nature* **281** 150-1

[9] Bonner WA, Lemmon RM and Noyes HP 1978 β radiolysis of crystalline ^{14}C-labeled amino acids. *J. Org. Chem.* **43** 522-4

[10] Bonner WA and Lemmon RM 1978 Radiolysis, racemization and the origin of optical activity. *Bioorg. Chem.* **7** 175-87

[11] Tokay RK, Norden B, Liljenzin JO and Andersson S 1986 Was natural β radioacitivity of carbon-14 the origin of optical one-handedness in life? *J. Radioanal. Nucl. Chem.* **104** 337-47

[12] Rosenberg RA, Abu Haija M and Ryan PJ 2008 Chiral-selective chemistry induced by spin-polarized secondary electrons from a magnetic substrate. *Phys. Rev. Lett.* **101** 178301

[13] Rosenberg RA 2011 Spin-polarized electron induced asymmetric reactions in chiral molecules. *Top. Curr. Chem.* **298** 279-306

[14] Mayer S, Nolting C and Kessler J 1996 Electron scattering from chiral molecules. *J. Phys. B* **29** 3497-511

[15] Nolting C, Mayer S and Kessler J 1997 Electron dichroism-new data and an experimental cross-check. *J. Phys.* B **30** 5491-9

[16] Christophorou LG, McCorkle DL and Christodoulides AA 1984 *Electron-Molecule Interactions and Their Applications* ed Christophorou LG (Orlando: Academic) p 477

[17] Stephen TM, Shi X and Burrow PD 1988 Temporary negative-ion states of chiral molecules: camphor and 2-methylcyclopentanone. *J. Phys. B: At. Mol. Opt. Phys.* **21** L169-71

[18] Aflatooni K and Burrow PD 2013 (private communication).

[19] Boudaffa B, Cloutier P, Hunting D, Huels MA and Sanche L 2000 Resonant formation of DNA strand breaks by low-energy (3 to 20 eV) electrons. *Science* **287** 1658-60

[20] Martin F, *et al.* 2004 DNA strand breaks induced by 0–4 eV electrons: the role of shape resonances. *Phys. Rev. Lett.* **93** 068101

[21] Abdoul-Carime H, Gohlke S and Illenberger E 2004 Site-specific dissociation of DNA bases by slow electrons at early stages of irradiation. *Phys. Rev. Lett.* **92** 168103

[22] Orlando TM, Oh D, Chen Y and Aleksandrov AB 2008 Low-energy electron diffraction and induced damage in hydrated DNA. *J. Chem. Phys.* **128** 195102

[23] Dreiling JM and Gay TJ 2014 Chirally sensitive electron-induced molecular breakup and the Vester-Ulbricht hypothesis. *Phys. Rev. Lett.* **113** 118103

[24] Dreiling JM, Burtwistle SJ and Gay TJ 2015 New technique for the reduction of helicity-correlated instrumental asymmetries in photoemitted beams of spin-polarized electrons. *Appl. Opt.* **54** 763-9

[25] Pierce DT, *et al.* 1980 The GaAs spin polarized electron source. *Rev. Sci. Instrum.* **51** 478-99

[26] Gay TJ, Furst JE, Trantham KW and Wijayaratna WMKP 1996 Optical electron polarimetry with heavy noble gases. *Phys. Rev. A* **53** 1623-9

[27] Arol Simpson J 1961 Design of retarding field energy analyzers. *Rev. Sci. Instrum.* **32** 1283-93

[28] Bevington PR and Robinson DK 1992 *Data Reduction and Error Analysis for the Physical Sciences*, (New York: McGraw Hill) p 58

[29] Scheer AM, Gallup GA and Gay TJ 2006 An investigation of electron helicity density in bromocamphor and dibromocamphor as a source of electron circular dichroism. *J. Phys. B: At. Mol. Opt. Phys.* **39** 2169-81

[30] Scheer AM, Gallup GA and Gay TJ 2008 Assignments of normally unoccupied orbitals to the temporary negative ion states of several lanthanide NMR shift reagents and comments on resonance involvement in electron circular dichroism. *J. Phys. Chem.* A **112** 4029-35